Genome Medicine

RESEARCH

Open Access

Novel multiplex family-wide PCR and Nanopore sequencing of amplicons (FP-NSA) approach for surveillance of influenza- and coronaviruses in humans and animals

Irene Kasindi Meki[1*], Ki Bum Ahn[1,2], William G. Dundon[1], Tirumala Bharani K. Settypalli[1], Christoph Leth[3], Adi Steinrigl[3], Sandra Revilla-Fernández[3], Friedrich Schmoll[3], Letizia Ceglie[4], Kouramoudou Berete[5], Artem Metlin[6], Madhur Dhingra[6], Norbert Nowotny[7,8], Giovanni Cattoli[1,4] and Charles Euloge Lamien[1]

Abstract

Background Recent outbreaks of zoonotic diseases like Ebola, Mpox, dengue fever, and COVID-19 highlight gaps in surveillance and early detection at disease hotspots. Virus family-wide diagnostic assays offer a cost-effective and sensitive alternative to metagenomics for initial virus identification. This study introduces a multiplex family-wide PCR coupled with Nanopore sequencing of amplicons (FP-NSA) for surveillance of novel and known zoonotic respiratory viruses, including influenza A and D viruses (IAV and IDV), alpha (α-), beta (β-), and gamma (γ-) coronaviruses (CoVs).

Methods This assay utilized primers in conserved regions of each virus group for multiplex reverse transcription (RT)-PCR coupled with the portable MinION device for rapid Nanopore sequencing. The FP-NSA was optimized using seven IAV subtypes, IDVs, and α- and β-CoVs. The analytical sensitivity of the FP-NSA was assessed using positive controls of known concentrations from each targeted viral family and validated using clinical samples and cell culture isolates from various host species and geographical origins. Potential novel viruses detected in the clinical samples, based on the FP-NSA, were further analyzed using metagenomics sequencing with the Sequence-Independent Single Primer Amplification (SISPA) approach.

Results The optimized FP-NSA assay efficiently detected all the targeted viruses singly as well as in co-infection scenarios of multiple respiratory viruses. Evaluation of the assay on 78 selected clinical and cell culture samples (from 184 initially screened) successfully detected IAVs; α-CoVs: porcine epidemic diarrhea virus (PEDV), human coronavirus (HCoV) NL63, and HCoV-229E; β-CoVs: HCoV-OC43, severe acute respiratory syndrome (SARS)-CoV-(1), SARS-CoV-2, and MERS-CoV; and γ-CoV infectious bronchitis virus (γ-CoV_IBV) infections. Additionally, the FP-NSA assay discovered a novel γ-CoV_IBV from Guinea that is phylogenetically distant from known genotypes using a SISPA metagenomics approach.

Conclusions The assay's short PCR amplicons enable screening of samples within 4 h, from PCR to sequencing and bioinformatics analysis, providing an adequate number of pathogens' reads. The portable MinION device makes

*Correspondence:
Irene Kasindi Meki
i.meki@iaea.org
Full list of author information is available at the end of the article

the assay suitable for pathogen surveillance in disease hotspots and resource-limited regions such as low- and middle-income countries. Thus, the FP-NSA assay is a valuable tool for detecting potential novel and known zoonotic respiratory viruses in the targeted families across various host species.

Keywords Zoonotic respiratory viruses, FP-NSA, Nanopore sequencing, Multiplex RT-PCR, Surveillance

Background

The majority of emerging and re-emerging human pathogens of significant public health concern worldwide are zoonotic, originate from domestic animals, wildlife, or arthropod vectors [1, 2]. Significant zoonotic pathogens belong to viral families such as Orthomyxoviridae, Coronaviridae, and Paramyxoviridae [3, 4]. Novel zoonotic viruses emerge through rapid mutation or reassortment of viruses from known families, driven by changes in environmental factors such as urbanization, which increase interactions between animal reservoirs and humans, leading to human transmission and potential epidemics or pandemics. On the other hand, the re-emergence of viral strains often results from limited public health prevention and control measures [5, 6].

Acute respiratory tract infections, mostly viral, cause over three million deaths annually worldwide. Emerging respiratory viruses such as coronaviruses [Middle East respiratory syndrome coronavirus (MERS-CoV), severe acute respiratory syndrome coronaviruses (SARS-CoV), and influenza A and B viruses] are WHO priority pathogens due to their potential to cause pandemics [3, 7]. Zoonotic respiratory virus infections such as those caused by influenza viruses and coronaviruses typically affect the upper respiratory tract, presenting similar symptoms like coughing, fever, runny nose, sneezing, and sore throat, and can lead to pneumonia and bronchiolitis [8].

Influenza viruses, with a segmented negative-stranded RNA genome, cause significant epidemics worldwide. There are 4 types of influenza viruses: influenza A virus (IAV), subtyped further based on two major antigens, haemagglutinin (HA) and neuraminidase (NA), infects birds and mammals; influenza B virus (IBV) infects mainly humans; influenza C virus (ICV) infects humans, pigs, and dogs; and influenza D virus (IDV) infects cattle, pigs, and humans [9]. Coronaviruses (CoVs), on the other hand, have a large positive-sense RNA genome and cause mild to severe respiratory illnesses. There are 4 genera of coronaviruses: alpha (α)-, beta (β)-, gamma (γ)-, and delta (δ)-coronaviruses. Alpha and beta CoVs mainly originate from bats, while gamma and delta CoVs are of avian origin. However, all CoVs can infect a range of mammalian species, including horses, cattle, camels, pigs, and rodents, which may serve as intermediate hosts prior to spillover to humans [10].

The rise in zoonotic disease outbreaks such as Ebola, Mpox, dengue, and COVID-19 highlights insufficient surveillance/testing capacity, especially in low-resource regions such as low- and middle-income countries or at disease hotspots such as high-density livestock operations or animals in trade. Effective surveillance approaches, particularly early detection at disease hotspots, are crucial to prevent pathogen spillover to humans [1, 5, 11, 12]. This requires deployable surveillance tools at national and regional levels to trace zoonotic pathogens at high-risk interfaces, therefore serving as an early warning system [13, 14].

Most of the conventional molecular methods applied in the surveillance of respiratory viruses such as PCR are designed based on known genomes, and as such, limit novel virus discovery. Next-generation sequencing (NGS) and third-generation sequencing (3GS) technologies such as PacBio and Oxford Nanopore Technology (ONT) aid not only in tracking disease transmission, but also in identifying emerging novel viral strains [11, 15]. Among these platforms, ONT library preparation is simple and rapid, easy to set up, and provides portable sequencing devices such as MinION that enables mobile sequencing with minimum training. Nevertheless, when applied to clinical samples, both NGS and 3GS can be very expensive, time-consuming, and data analysis requires a high level of expertise, especially due to host-derived contaminants. Moreover, the sensitivity can be low if no pathogen enrichment procedure is applied when the pathogen load is too low, making them less suitable for disease surveillance in low-resource settings [11, 16].

Therefore, effective strategies/tools for the timely detection and surveillance of emerging and re-emerging zoonotic pathogens at the animal-human interface are required. Given that most of the recent novel emerging viruses originated from the above-mentioned viral families, family-based approaches offer more sensitive alternatives to metagenomics in detecting new variants and viral family members [17–20]. Here, we propose a multiplex family-wide PCR and Nanopore sequencing of amplicons (FP-NSA) tool as an alternative approach for surveillance of zoonotic respiratory viruses belonging to influenza and coronavirus families.

Methods

Target gene selection and primer design

The full-length sequences of the most conserved RNA-dependent RNA polymerase (ORF1ab) gene of Coronaviridae, α-CoV and β-CoV (41 sequences), and the matrix (M) gene sequences of Orthomyxoviridae, IAV (141 sequences) and IDV (58 sequences), were downloaded from GenBank and aligned using BioEdit (v7.2.6). Each targeted gene dataset contained sequence representatives of virus strains from different geographical locations and host species. The consensus sequence of the conserved region of each alignment was used to design primers specific for each virus family/genus using Primer3Plus (Additional file 1: Table s1) [21]. BLAST searches to evaluate the primer specificity showed that the α- and β-CoV primer set could equally detect the γ-CoVs. The primers were ordered from Eurofins Genomics, Ebersberg, Germany.

Samples, nucleic acid extraction, and positive controls

The RNA positive controls used for optimizing each targeted virus detection included: α-CoVs: transmissible gastroenteritis virus (TGEV) and porcine epidemic diarrhea virus (PEDV), provided by the Department for Molecular Biology at the Austrian Agency for Veterinary Disease Control Mödling (AGES); α-CoV human coronavirus 229E (HCoV-229E), and β-CoVs SARS-CoV-(1) and SARS-CoV-2 purchased from Vircell, Spain; MERS-CoV provided by the University of Veterinary Medicine Vienna (Vetmeduni); IAV subtypes H1N1, H3N8, H3N2, H5N1, H7N7, H9N2, and H16N3 and IDVs, Infl-D L6/17 and Infl-D L1/19, kindly provided by Istituto Zooprofilattico Sperimentale delle Venezie (IZSVe), Padova, Italy. Total RNA of the clinical samples included in this study was extracted using the RNeasy Mini kit (Qiagen) following standard procedures. The samples originated from 15 countries and 12 host species, as detailed in the assay validation section and in Additional file 1: Table s2.

Multiplex reverse transcription (RT)-PCR optimization

The primers for each virus group were first optimized in singleplex reactions to determine a suitable annealing temperature and optimal primer concentration. The primer sets were then pooled for a multiplex reaction, optimizing concentrations with templates from each virus family or a mixture of viruses from different families per reaction. The final optimized conditions for the multiplex RT-PCR assay were 20 µl reaction volume containing 4 µl of One-Step RT-PCR Buffer 5X (Qiagen), 0.8 µl One-Step RT-PCR enzyme mix, a final concentration of 900 nM of each of the forward and reverse primers of α-, β-, and γ-CoVs, 100 nM of each of the forward and reverse primers of IAV and IDV, and 2 µl of the RNA template. Optimal PCR cycling conditions consisted of reverse transcription at 50 °C for 30 min, initial denaturation at 95 °C for 15 min, followed by 40 cycles of 94 °C for 30 s, 52 °C for 30 s, and 72 °C for 30 s, and final extension at 72 °C for 10 min.

Determination of sensitivity and limit of detection (LoD) of the FP-NSA

The limit of detection (LoD) of the FP-NSA was determined by performing multiplex RT-PCR on 10-fold serial dilutions of RNA derived from clinical and cell culture isolates of H5N1 (IAV), Infl-D L6/17 (IDV), and SARS-CoV-2 (CoV). These RNA samples were initially quantified by real-time quantitative PCR (RT-qPCR) as described in Additional file 1: Methods s1. For Nanopore sequencing, 2 µl of PCR product generated from each dilution was used for library preparation following the protocol outlined in Additional file 1: Methods s2. The assay's sensitivity or the LoD was defined as the highest quantification cycle (Cq) value for each viral target that resulted in a visible amplification band of the expected size by multiplex RT-PCR and generated sufficient viral sequence reads exceeding the predetermined read count threshold.

Validation and specificity evaluation of the FP-NSA assay

The performance of the FP-NSA assay in detecting the selected respiratory zoonotic viruses was evaluated by initially screening RNA extracted from 184 clinical samples and cell culture isolates using multiplex RT-PCR, followed by sequencing and analysis of a subset of 78 of the amplicons (Fig. 1; Additional file 1: Table s2). The clinical samples included 100 avian samples from various countries, 5 beaver samples from a conservation farm in Mongolia, 2 human samples provided by the Korea Atomic Energy Research Institute (KAERI), Korea, 35 samples from swans, a greylag goose, chicken, humans, and a domestic pig provided by AGES, and 8 cell culture supernatant samples which were part of a MERS-CoV proficiency testing (PT) panel [22], provided by Vetmeduni, Vienna, Austria. The avian samples from different countries had been previously tested for IAV using a duplex RT-qPCR [23], while the beaver samples were confirmed SARS-CoV-2-positive using RT-qPCR by Takemura et al. [24]. The samples from AGES had been tested for PEDV using the Tetracore PED/TGE/PDCoV RT-qPCR assay (Tetracore, Inc.), IAV by the RT-qPCR according to Hoffmann et al. [25], γ-CoV_IBV using the RT-qPCR adapted from Muradrasoli et al. [26], and SARS-CoV-2 using the LightMix® Modular E-gene qPCR Kit (TIB MolBiol, Berlin, Germany). The MERS-CoV PT panel samples were tested using RT-qPCR assays described by Corman et al. [27].

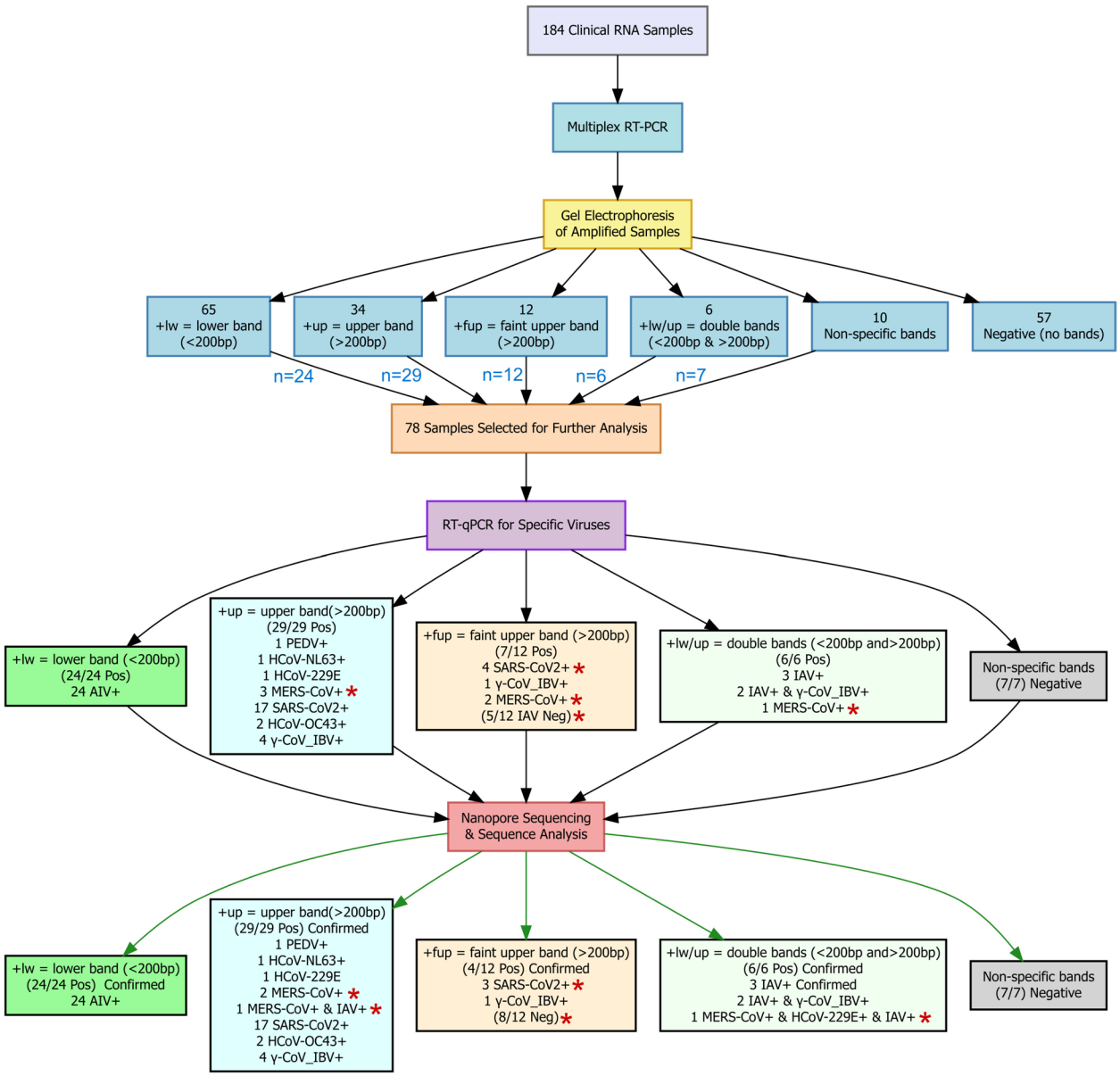

Fig. 1 Flow chart overview of the FP-NSA assay validation. Illustrates the selection of 78 representative samples from a total of 184 clinical samples and cell culture isolates, and their comparison with RT-qPCR screening results. Samples showing discrepancies between FP-NSA and RT-qPCR are marked with asterisks

The assay's specificity or potential cross-reactivity was evaluated with RNA from 10 peste des petits ruminants virus (PPRV)-positive goats, 9 rabies virus (RABV)-positive bovine samples, and 15 avian paramyxovirus 1 (APMV-1)-positive chickens. Representative clinical samples presenting different amplification patterns were further analyzed by Nanopore sequencing technology (Fig. 1).

Preparation of Nanopore sequencing libraries

Amplicons were purified using the PCR clean-up system kit (Promega) and sequenced using the Nanopore MinION device. Libraries of the purified PCR products were prepared using the Amplicon by Ligation Kit (SQK-LSK109) and the Native Barcoding Expansion kit (EXP-NBD104) or SQK-NBD114.24 kit following ONT standard protocols (details in Additional file 1: Methods s2).

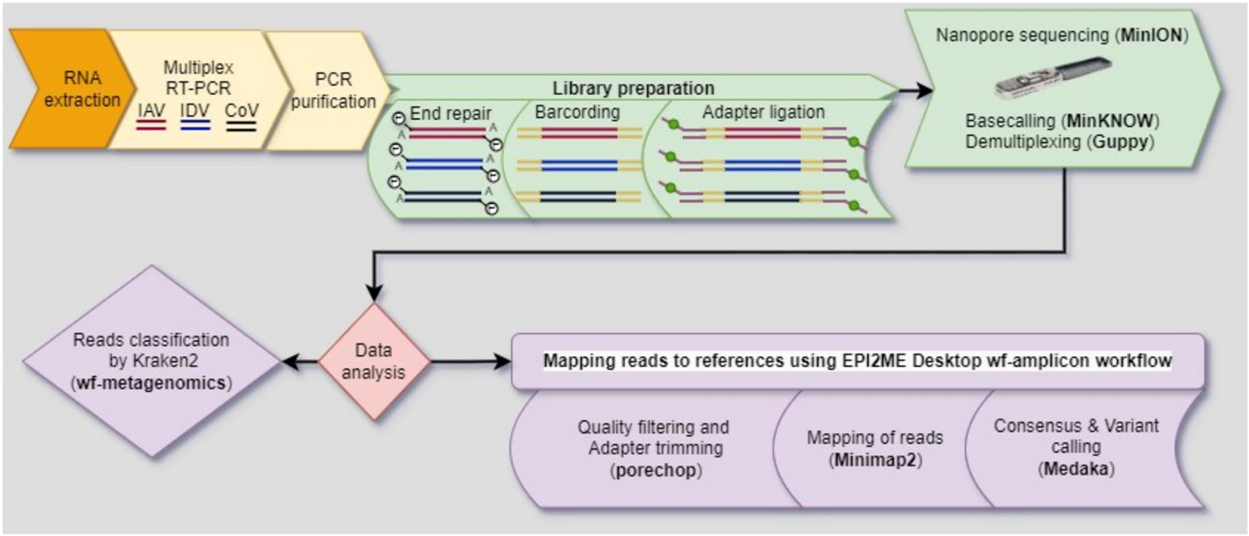

Fig. 2 Step by step workflow for simultaneous detection and sequencing of selected zoonotic respiratory viruses. The workflow includes sample processing (RNA extraction, One-Step RT-PCR and purification), library preparation and Nanopore sequencing and data analyses

Nanopore sequencing data analysis

The generated fastq data was first analyzed following the Nanopore wf-metagenomics workflow with Kraken2 for read classification, with read length cut-off set to minimum 150 bp to maximum 350 bp and minimum read quality set to 8 [28]. Misassigned reads during demultiplexing were subtracted from each sample based on the NTC maximum read count of each targeted virus. The consensus sequences of the amplified pathogens were retrieved following the Nanopore amplicon analysis workflow (wf-amplicon). The workflow involves filtering the low-quality and short reads and trimming the adapters using porechop (v0.2.4). The cleaned reads were mapped against the reference sequences of the targeted regions of each virus family: HCoV-229E (NC_002645), PEDV (NC_003436), HCoV-NL63 (NC_005831), SARS-CoV-1 (JX163923), SARS-CoV-2 (NC_045512), MERS-COV (NC_019843), HCoV-OC43 (NC_006213), γ-CoV_IBV_MK204393, IAV_AF348188, and IDV_LC522356, using minimap2 (v2.26). Variant calling and consensus sequences were generated with the medaka program (v1.9.1). The quality of the mapped sorted reads was also assessed by QualiMap v2.3, and the consensus sequences were aligned and visualized with a reference sequence of each virus using BioEdit (v7.2.6). An overview of the workflow for amplicon-based Nanopore sequencing for surveillance of selected respiratory zoonotic viruses is illustrated in Fig. 2. The Nanopore wf-metagenomics and wf-amplicon workflow analysis was compared to an in-house bash script-based analysis (Additional file 1: Methods s3).

Correlation of the real-time quantitative RT-qPCR and the FP-NSA

The correlation between the FP-NSA assay and the RT-qPCR was assessed using Fleiss' kappa test on categorical data (positive or negative) of the 78 selected samples using the Interrater Reliability (irr) package in R.

Metagenomics sequencing and analysis of IBV-infected chicken sample

Following the analysis of the clinical samples using the FP-NSA, two γ-CoV_IBV positive samples with low nucleotide sequence identities based on NCBI BLAST search (s66 and s68) were selected for metagenomics sequencing by the Sequence-Independent Single Primer Amplification (SISPA) approach [29]. Details of the SISPA protocol are provided in Additional file 1: Methods s4.

The obtained γ-CoV IBV genome was aligned with other γ-CoV genome sequences retrieved from GenBank using MAFFT. A maximum likelihood phylogenetic tree was created using RAxML v2.0.6, based on the complete γ-CoV_IBV Spike (S) gene, and visualized on the Interactive Tree of Life (ITOL) tool [30].

Results

Multiplex RT-PCR of respiratory zoonotic viruses

The preliminary singleplex RT-PCR assays to detect viruses from different families generated clear single target-specific amplicons (Fig. 3A). Following several optimization attempts, the final multiplex RT-PCR conditions were set at 52 °C annealing temperature with a final concentration of 900 nM of the CoV primers and

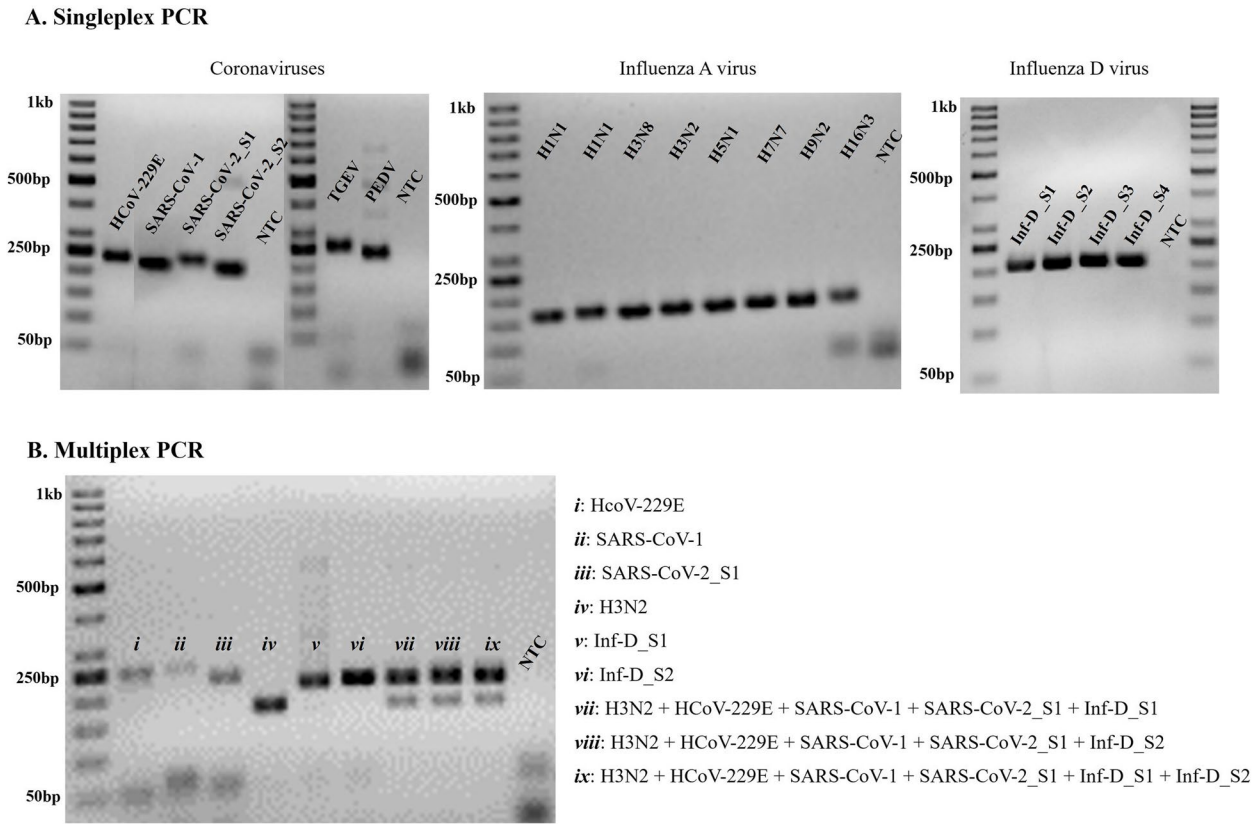

Fig. 3 Gel electrophoresis images showing the amplification pattern of α- and β-CoVs, IAVs, and IDVs in **A** singleplex RT-PCR and **B** multiplex RT-PCR conditions

100 nM of the IAV and IDV primers. These conditions produced amplicons of the expected sizes of all targeted viruses, with minimal background and without cross-amplification (Fig. 3B). Moreover, the multiplex RT-PCR effectively detected multiple viruses in co-infection scenarios by mixing RNA samples positive for different viruses, resulting in double-band patterns consistent with the simultaneous amplification of multiple targets (Fig. 3B, lane *vii*, *viii*, and *ix*).

Limit of detection and sensitivity of the FP-NSA assay

To establish the sensitivity and the LoD of the FP-NSA, serially diluted representative clinical samples from each viral family were analyzed in parallel using RT-qPCR. The assay successfully detected H5N1 (IAV) at a Cq value > 40, Infl-D L6/17 (IDV) at 33.0, and SARS-CoV-2 (CoV) at 32.4, with each dilution producing a visible amplification band of the expected size that yielded over 1000 viral sequence reads. Additionally, a SARS-CoV-2 sample with a Cq value of 35.4 produced a faint band that generated 689 viral sequence reads, which exceeded the predefined minimum sequence read number threshold for the LoD (Fig. 4).

Analysis of RT-PCR amplicons by Nanopore sequencing

The ability of the FP-NSA to detect multiple respiratory viruses simultaneously was assessed by sequencing PCR products of a sample containing CoVs, IAV, and IDV (Fig. 3B, sample *ix*). After cleaning the raw read sequences of sample *ix* by removing low-quality reads and the adaptors, 176,526 reads were analyzed and classified by Kraken2 on Nanopore wf-metagenomics as well as wf-amplicon; 20,500 reads were mapped to IAV (12.8%), 105,900 to IDV (66.1%), 14,800 to α-CoV (9.2%), and 19,100 to β-CoV (12%). These proportions matched the intensity of the multiplex RT-PCR product bands (Fig. 3B, sample *ix* and Fig. 5A). Mapping of the clean reads against the reference sequences of the targeted regions of each virus family showed a high coverage along the amplicon length for each pathogen (Fig. 5B–F). These results were similar to those obtained using the in-house bash script analysis (data not shown).

Validation of the FP-NSA assay for surveillance of respiratory zoonotic viruses

The performance of the FP-NSA assay was evaluated using 184 clinical samples and cell culture isolates from

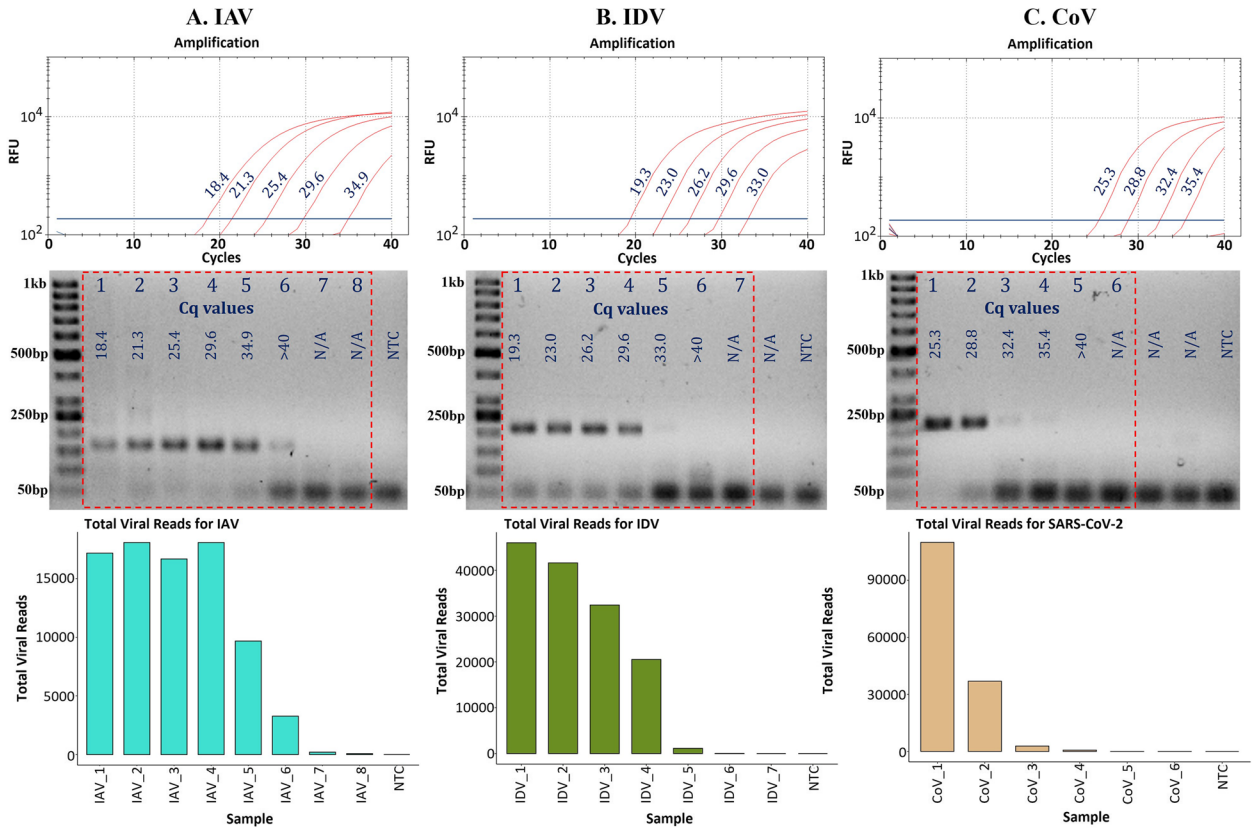

Fig. 4 Limit of detection (LoD) of FP-NSA for **A** IAV (Cq, > 40), **B** IDV (Cq, > 33.0), and **C** CoV (Cq, > 32.4) compared to RT-qPCR

various host species and geographical origins (Fig. 1). Gel electrophoresis analysis of the multiplex RT-PCR products revealed distinct target-specific amplicon sizes: 65 samples showed bands < 200 bp, indicative of IAV; 46 samples showed bands > 200 bp, consistent with CoVs; and 6 samples exhibited both bands, suggesting IAV and CoV co-infections. No amplification or only faint non-specific bands were observed in 67 samples, including those positive for RABV in bovine and PPRV in goats (Additional file 1: Fig. s1). To further characterize the successfully amplified samples, 78 samples (s1–s78) representing various amplification patterns (24: lower band < 200 bp, 41: upper band > 200 bp, 6: double bands < 200 bp + > 200 bp, and 7 non-specific bands) were sequenced using ONT on a MinION device (Fig. 1; Additional file 1: Fig. s1).

Sequence read analysis of the 78 samples using Nanopore workflows (wf-metagenomics and wf-amplicon) confirmed IAV in all 24 samples with lower bands. Among the 41 samples presenting upper bands, sequence analysis identified: α-CoVs in 3 samples: PEDV, HCoV-NL63, and HCoV-229E, β-CoVs in 25 samples: 2 HCoV-OC43, 20 SARS-CoV-2, 3 MERS-CoV, including one co-infection with IAV, and γ-CoV_IBV in 5 samples. Among the samples showing faint upper bands, 5 of these [a chicken sample (s5) from Cameroon and four Cape cormorant samples (s16–s19) from Namibia] were confirmed negative for the targeted viruses by Nanopore sequencing, indicating false positive bands, while 2 MERS-CoV samples (s74 and s75) and 1 SARS-CoV-2 sample (s43) yielded insufficient viral reads despite being RT-qPCR positive. Among the 6 samples with double bands, sequencing confirmed co-infections of IAV and γ-CoV_IBV in 2 samples (s64 and s67) and IAV with MERS-CoV and HCoV-229E in 1 sample (s76), and IAV alone in the remaining 3 samples (s13–s15). No viral reads were detected in any of the seven samples with non-specific bands (s54–s60) (Table 1, Fig. 6A–D). Samples with read counts below the set threshold were considered negative for the targeted viruses. While the total sequence reads produced in most of the samples ranged between 10 and 100 k, most samples showed a relatively high number of the targeted viral reads per 4 k of the total sequence reads, ranging from 1200 to 3900 reads. Exceptions included two γ-CoV_IBV positive samples, s37 from AGES (with a faint band) and s66 from Botswana, that had 73 and 367 γ-CoV_IBV reads, respectively. In comparison to

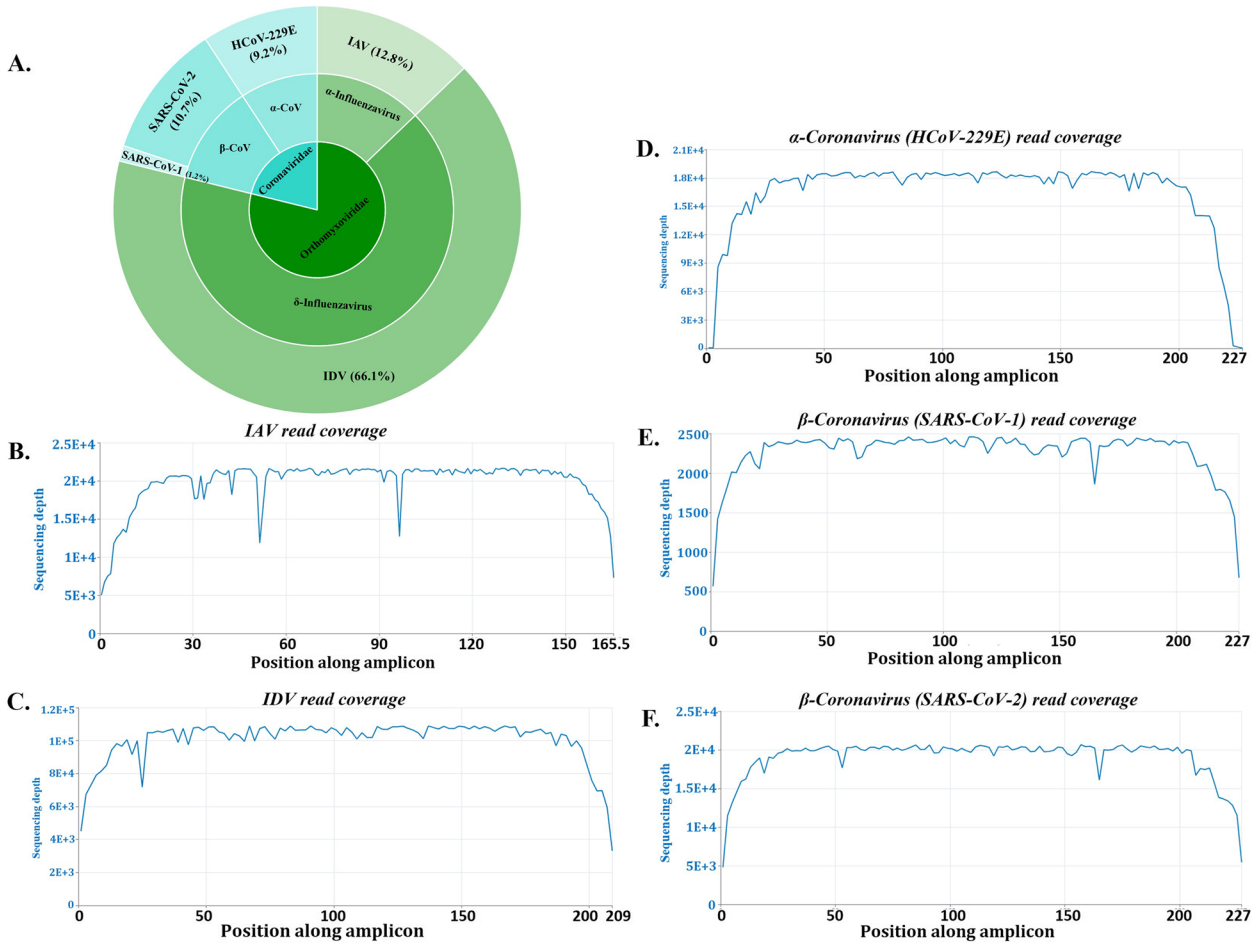

Fig. 5 Sequencing analysis of a sample presenting multiple bands (co-infection). **A** Proportions of sequence reads from sample *ix* (Fig. 3B), as classified by the Nanopore wf-metagenomics and wf-amplicon. **B-F** Overview of the mapping quality and coverage of the clean reads against the reference sequences

the RT-qPCR Cq values, the sequence approach demonstrated high sensitivity in detecting the targeted respiratory viruses across any given Cq value: IAV (Cq < 32), α- and β-CoVs (Cq < 30), and γ-CoV_IBV (Cq < 32), with the exception of three samples, s43 (Cq 28, SARS-CoV-2), s74 (Cq 30.7, MERS-CoV), and s75 (Cq 36.2, MERS-CoV) (Fig. 6, Table 1). Moreover, the agreement between the RT-qPCR and FP-NSA in the 78 clinical samples was evaluated using Fleiss kappa, yielding a coefficient (k) value of 0.866 (*P* value of 2.09e − 14), indicating strong concordance between the two methods.

Whole genome analysis of γ-CoV infectious bronchitis virus

Among the clinical samples analyzed by the FP-NSA assay, a BLAST search using the short amplicon reads showed that s66 and s68 γ-CoV_IBV samples had a low similarity to the publicly available sequences. SISPA metagenomics sequencing of these two samples revealed the presence of retroviruses (93%), Orthobunyavirus Schmallenberg (3%), picornaviruses (1%), and coronaviruses (< 1%) in sample s66 from Botswana and retroviruses (77.3%), Orthobunyavirus Schmallenberg (8%), and coronaviruses (14%) in sample s68 from Guinea, using the Centrifuge tool (Additional file 1: Fig. s2). The Sequence Read Archive (SRA) data for both samples have been submitted to GenBank under BioSample accession numbers SAMN51157819 and SAMN51157820.

BLAST search of the extracted corresponding viral reads identified by the Centrifuge tool, using an in-house script, confirmed the identities of the γ-CoV_IBV reads in each sample. Sample s66 did not yield adequate γ-CoV_IBV reads (1220 reads) for whole genome assembly; however, a partial γ-CoV_IBV genome of 24,062 bp was obtained from sample s68 assembly with a mean coverage of 246.18 and mean mapping quality of 58.84 (GenBank accession number: PQ553913). The s68 γ-CoV_IBV partial genome included open reading

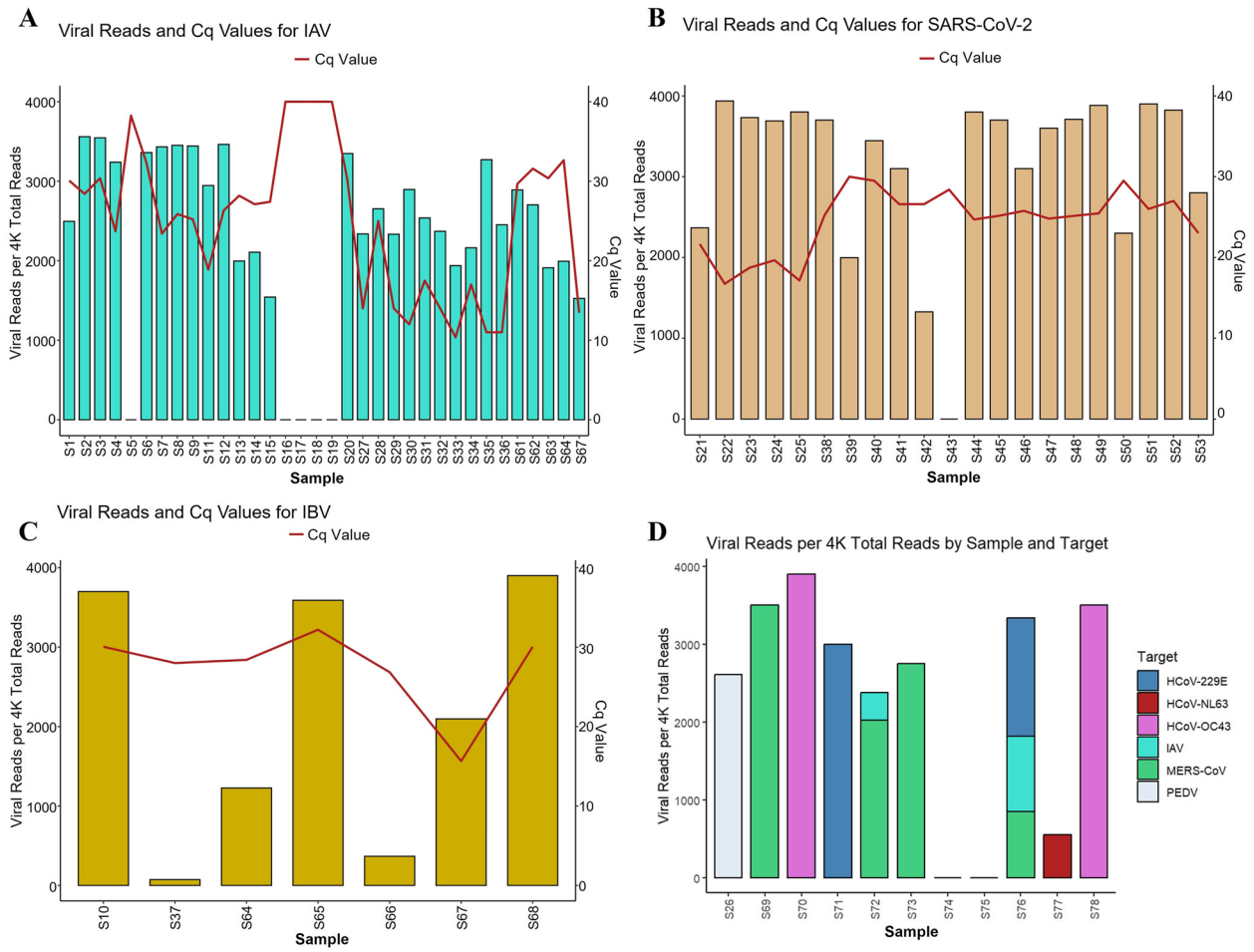

Fig. 6 Average number of mapped viral reads per 4000 of the total sequence reads of the sequenced clinical samples, plotted against the RT-qPCR Cq values for **A** IAV, **B** SARS-CoV-2, and **C** IBV. **D** Viral read counts from other sequenced samples included in the study

frames (ORFs) encoding coronavirus polyprotein 1ab and spike (S) protein. NCBI nucleotide blast search based on the s68 γ-CoV_IBV partial genome showed 77.94% identity (query coverage: 62%) to a Chinese IBV strain (KX302866.1) and 77.41% (query coverage: 64%) to a Mexican IBV isolate (OR268749.1_Mex-14P). Phylogenetic analysis based on the complete spike gene of S68_IBV_Guinea with other γ-CoVs retrieved from GenBank clustered the Guinea isolate separate from known γ-CoV_IBV genotypes reported in Africa (GI lineages) as well as the above-mentioned Chinese isolate_KX302866.1 (QX-like). However, the Guinea IBV isolate clustered with γ-CoV_IBV isolates from the USA (OP381188.1_GVIII-1), the UK (MN548286.1_GII-1), and Georgia_USA vaccine (GQ504723_GIV-1), with the closest being GIX-1 isolates from Mexico (OR268749.1 and OR268750.1) (Fig. 7).

Discussion

This study introduces a virus family-based multiplex RT-PCR, coupled with Nanopore sequencing (FP-NSA) as a user-friendly and field-adaptable tool/approach for surveillance of known and potential novel zoonotic respiratory viruses belonging to IAV, IDV, and α-, β-, and γ-CoVs. The development of the assay exploited the conserved genomic regions of the targeted virus families to generate short amplicons (160–250 bp), thereby enhancing detection sensitivity, particularly from clinical samples with low RNA integrity. The integration with rapid Nanopore sequencing using the portable MinION device offers an advantage over other NGS platforms [31–35].

The FP-NSA assay successfully detected various targeted pathogens including diverse IAV subtypes, IDVs, and α-, β-, and γ-CoVs, even in co-infected samples. The specificity of the assay was demonstrated by the absence of amplification of unrelated viruses such as RABV and PPRV, while the false positives observed as faint bands

Table 1 Nanopore MinION sequencing results of selected clinical samples. N/D = not detected, + lw = lower band (< 200 bp), + up = upper band (> 200 bp), + lw/up = double bands (< 200 bp and > 200 bp), + fup = faint upper band (> 200 bp), and N/S + Non-specific bands

Sample	Host species	Pathogen tested previously by RT-qPCR (Cq value)	Multiplex Family-wide PCR	Mapped viral reads per 4k total sequence reads							
				IAV	α-CoV			β-CoV			γ-CoV
					PEDV	HCoV-229E	HCoV-NL63	SARS-CoV-2	MERS-CoV	HCoV-OC43	IBV
S1-Mauritania	White pelican	IAV (30.1)	$+^{lw}$	2495							
S2-Lesotho	Poultry (chicken)	IAV (28.4)	$+^{lw}$	3560							
S3-Lesotho	Poultry (chicken)	IAV (30.4)	$+^{lw}$	3546							
S4-Botswana	Poultry (chicken)	IAV (23.7)	$+^{lw}$	3239							
S5-Cameroon	Poultry (chicken)	IAV (N/D)	$+^{fup}$								
S6-Cameroon	Poultry (chicken)	IAV (32.3)	$+^{lw}$	3360							
S7-Cameroon	Poultry (chicken)	IAV (23.4)	$+^{lw}$	3432							
S8-Guinea	Poultry (chicken)	IAV (25.9)	$+^{lw}$	3451							
S9-Guinea	Poultry (chicken)	IAV (25.2)	$+^{lw}$	3443							
S10-Guinea	Poultry (chicken)	IAV/ γ-CoV IBV (N/D/30.1)	$+^{up}$								3700
S11-Vietnam	Duck	IAV (18.9)	$+^{lw}$	2946							
S12-Kenya	Poultry (chicken)	IAV (26.3)	$+^{lw}$	3463							
S13-Namibia	Cape cormorant	IAV (28.2)	$+^{lw/up}$	1996							
S14-Namibia	Cape cormorant	IAV (27.1)	$+^{lw/up}$	2107							
S15-Namibia	Cape cormorant	IAV (27.4)	$+^{lw/up}$	1542							
S16-Namibia	Cape cormorant	IAV (N/D)	$+^{fup}$								
S17-Namibia	Cape cormorant	IAV (N/D)	$+^{fup}$								
S18-Namibia	Cape cormorant	IAV (N/D)	$+^{fup}$								
S19-Namibia	Cape cormorant	IAV (N/D)	$+^{fup}$								
S20-Namibia	Cape cormorant	IAV (30.2)	$+^{lw}$	3348							
S21-Mongolia	Beaver	SARS-CoV-2 (21.7)	$+^{up}$					2367			
S22-Mongolia	Beaver	SARS-CoV-2 (16.7)	$+^{up}$					3937			
S23-Mongolia	Beaver	SARS-CoV-2 (18.7)	$+^{up}$					3731			
S24-Mongolia	Beaver	SARS-CoV-2 (19.7)	$+^{up}$					3690			
S25-Mongolia	Beaver	SARS-CoV-2 (17.2)	$+^{up}$					3801			
S26-AGES	Domestic pig	PEDV (16.0)	$+^{up}$		2611						
S27-AGES	Swan	IAV (14.0)	$+^{lw}$	2337							
S28-AGES	Mute swan	IAV (25.0)	$+^{lw}$	2653							
S29-AGES	Swan	IAV (14.0)	$+^{lw}$	2333							
S30-AGES	Mute swan	IAV (12.0)	$+^{lw}$	2896							
S31-AGES	Mute swan	IAV (17.5)	$+^{lw}$	2538							
S32-AGES	Swan	IAV (14.0)	$+^{lw}$	2370							
S33-AGES	Greylag goose	IAV (10.37)	$+^{lw}$	1938							
S34-AGES	Mute swan	IAV (17.0)	$+^{lw}$	2162							
S35-AGES	Mute swan	IAV (11.0)	$+^{lw}$	3271							
S36-AGES	Mute swan	IAV (11.0)	$+^{lw}$	2452							
S37-AGES	Poultry (chicken)	γ-CoV IBV (28.0)	$+^{fup}$								73
S38-AGES	Human	SARS-CoV-2 (25.2)	$+^{up}$					3700			
S39-AGES	Human	SARS-CoV-2 (30.0)	$+^{fup}$					1997			
S40-AGES	Human	SARS-CoV-2 (29.5)	$+^{up}$					3445			
S41-AGES	Human	SARS-CoV-2 (26.6)	$+^{up}$					3100			
S42-AGES	Human	SARS-CoV-2 (26.6)	$+^{up}$					1326			
S43-AGES	Human	SARS-CoV-2 (28.4)	$+^{fup}$								
S44-AGES	Human	SARS-CoV-2 (24.7)	$+^{up}$					3800			
S45-AGES	Human	SARS-CoV-2 (25.2)	$+^{up}$					3700			
S46-AGES	Human	SARS-CoV-2 (25.8)	$+^{up}$					3100			
S47-AGES	Human	SARS-CoV-2 (24.8)	$+^{up}$					3600			
S48-AGES	Human	SARS-CoV-2 (25.2)	$+^{up}$					3710			
S49-AGES	Human	SARS-CoV-2 (25.5)	$+^{up}$					3882			
S50-AGES	Human	SARS-CoV-2 (29.5)	$+^{fup}$					2300			
S51-AGES	Human	SARS-CoV-2 (26.0)	$+^{up}$					3900			
S52-AGES	Human	SARS-CoV-2 (27.0)	$+^{up}$					3824			
S53-AGES	Human	SARS-CoV-2 (23.0)	$+^{fup}$					2800			
S54-Ethiopia	Goat	PPRV	N/S								
S55-Ethiopia	Goat	PPRV	N/S								
S56-Ethiopia	Goat	PPRV	N/S								
S57-Ethiopia	Goat	PPRV	N/S								
S58-Ethiopia	Goat	PPRV	N/S								
S59-Ethiopia	Goat	PPRV	N/S								
S60-Ethiopia	Goat	PPRV	N/S								
S61-Kuwait	Chicken	IAV/ APMV-1 (29.7/N/D)	$+^{lw}$	2891							
S62-Kuwait	Chicken	IAV/ APMV-1 (31.6/N/D)	$+^{lw}$	2703							
S63-Kuwait	Chicken	IAV/ APMV-1 (30.4/N/D)	$+^{lw}$	1911							
S64-Ivory coast	Chicken	IAV/ γ-CoV IBV (32.6/28.4)	$+^{lw/up}$	1993							1227
S65-Ivory coast	Chicken	γ-CoV IBV (32.2)	$+^{up}$								3590
S66-Botswana	Chicken	γ-CoV IBV (26.9)	$+^{up}$								367
S67-Kuwait	Chicken	IAV/ γ-CoV IBV (13.4/15.7)	$+^{lw/up}$	1426							2097
S68-Guinea	Chicken	γ-CoV IBV (30.1)	$+^{up}$								3900
S69-Vetmeduni	MERS-CoV PT-panel	MERS-CoV (27.8)	$+^{up}$						3502		
S70-Vetmeduni	MERS-CoV PT-panel	HCoV-OC43 (27.9)	$+^{up}$							3900	
S71-Vetmeduni	MERS-CoV PT-panel	HCoV-229E (28.0)	$+^{up}$			3000					
S72-Vetmeduni	MERS-CoV PT-panel	MERS-CoV (27.7)	$+^{up}$	356					2022		
S73-Vetmeduni	MERS-CoV PT-panel	MERS-CoV (26.2)	$+^{up}$						2752		
S74-Vetmeduni	MERS-CoV PT-panel	MERS-CoV (30.7)	$+^{fup}$								
S75-Vetmeduni	MERS-CoV PT-panel	MERS-CoV (36.2)	$+^{fup}$								
S76-Vetmeduni	MERS-CoV PT-panel	MERS-CoV (28.5)	$+^{lw/up}$	966		1518			851		
S77-KAERI	Human	HCoV-NL63 (30.0)	$+^{up}$				551				
S78-KAERI	Human	HCoV-OC43 (21.9)	$+^{up}$							3500	

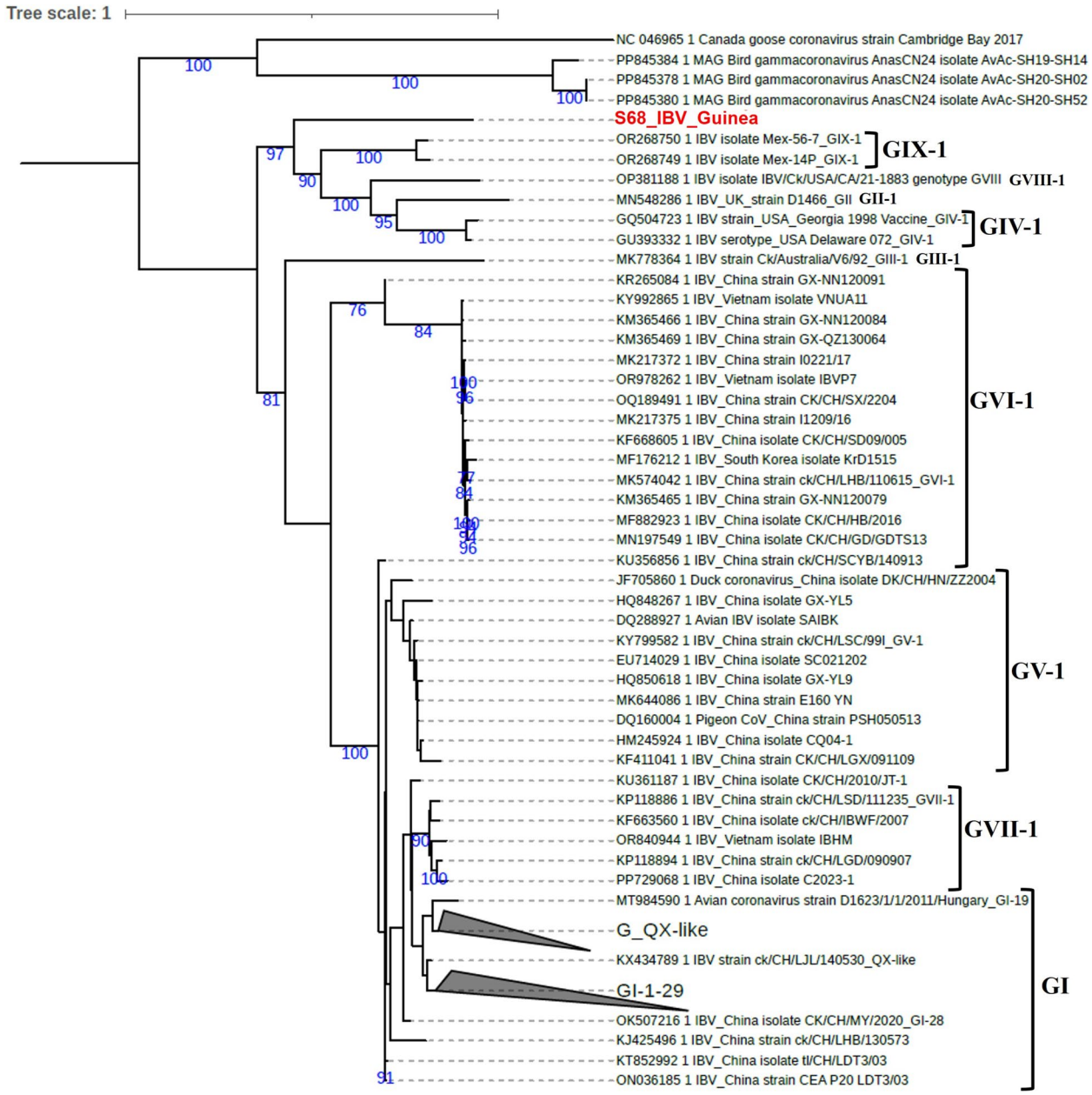

Fig. 7 Maximum likelihood phylogenetic tree of γ-CoV infectious bronchitis virus (IBV) based on the complete S gene, using a total of 220 sequences including the γ-CoV_IBV isolate from Guinea (highlighted in red). The evolutionary distances were computed using the GTR model with gamma distribution and invariant sites. The tree was visualized on iTOL with all 8 γ-CoV_IBV genotypes represented

in the multiplex RT-PCR were resolved by sequencing, underscoring the importance of sequence validation to ensure diagnostic precision.

While singleplex RT-PCR is generally considered more sensitive with higher reproducibility compared to multiplex RT-PCR [36], the FP-NSA demonstrated comparable sensitivity. The assay successfully detected IAV, IDV, and SARS-CoV-2 at Cq values of > 40, 33.0, and 32.4, respectively—each producing expected amplification bands and over 1000 viral sequence reads. Notably, a SARS-CoV-2 sample with a Cq of 35.4 presented a faint band but still generated 689 reads, demonstrating the assay's capacity to detect low viral loads. Screening of 184 clinical and cell culture samples from different hosts and locations, followed by sequencing of 78 representative samples, confirmed the presence of the targeted viruses,

with the results closely aligning with the initial RT-qPCR screening. Notable discrepancies were observed in two MERS-CoV samples with high Cq values (> 30) and 1 SARS-CoV-2 sample which presented a faint band and yielded insufficient viral reads, likely as a result of a high level of degeneracy in the CoV primers or the use of a different set of primers in the RT-qPCR [37].

A notable outcome of this study was the discovery of a novel γ-CoV_IBV in two samples. By employing a SISPA metagenomics sequencing approach on these two samples, one partial γ-CoV_IBV genome was obtained from the chicken sample from Guinea, with significant genetic divergence from known IBV genotypes. However, the identified γ-CoV_IBV from Guinea was genetically close to genotype GIX-1 isolated in Mexico, where IBV genotypes with great variability (such as GI-1 and GI-9, or extreme divergent like GI-30, GVIII-1, and GIX-1) have been described [38]. Although there are vaccination programs in Guinea against γ-CoV_IBV, the sample analyzed in this study was collected from a farm affected by an avian influenza outbreak, where no vaccination against γ-CoV_IBV had been implemented. This discovery demonstrates the capability of the FP-NSA assay in detecting both known and novel viruses in the targeted groups across hosts, including IAV in birds and humans, and SARS-CoV-2 in humans and beavers [9, 10].

The FP-NSA offers several key advantages: the single set of primers employed in the multiplex RT-PCR not only targets a single virus, but multiple virus family members, thus expanding the discovery and surveillance of novel viruses in the targeted viral families simultaneously. This is an improvement on the more labor-intensive pan-viral surveillance assays that rely on nested or semi-nested PCR assays that require multiple primer sets, with a higher risk of cross-contamination [17–19]. The multiplex approach is cost-effective, time-saving, and requires low sample input [12, 39–42]. Due to the targeted short amplicons, the assay provides rapid processing, from PCR to sequencing and data analysis, and the 4 k reads/sample file acquired within 30 min of sequencing 12 multiplexed/pooled samples produces adequate numbers of reads (> 1000), ensuring reliable identification of the amplified pathogens. Moreover, in comparison to other sequencing platforms, ONT library preparation is simple and scalable, and provides real-time data streaming with high yields and offers user-friendly data analysis pipelines that require minimal training/experience [43]. Most importantly, the portable MinION device enables mobile sequencing, which is crucial for disease surveillance in hotspot areas such as high-density livestock operations or animals in trade where high pathogen prevalence is likely [44–46]. Although not tested in this study, the developed multiplex RT-PCR can also be optimized for portable PCR machines which are currently used in outdoor or point-of-care diagnostics for infectious diseases [47].

Despite these strengths, the FP-NSA has limitations, including the need for cold chain management and technical precision in library preparation, RNA extraction, and reverse transcription steps posing logistical challenges for point-of-care use. Though the cost of Nanopore sequencing can be as low as $0.60/sample, depending on the flow cell usage and level of multiplexing, compared to other NGS platforms, initial investments and operational costs may still be limiting for some low-income settings [48]. Effective implementation of the method requires moderate capacity building, including personnel training, infrastructure, and data analysis capabilities [49]. Efforts to address gaps in disease surveillance include capacity-building initiatives like the VETLAB network and the IAEA's ZODIAC program. These initiatives support national laboratories through group training at the FAO/IAEA Animal Production and Health Laboratory in Seibersdorf, Austria, and in-country visits to assist veterinary staff in applying advanced tools alongside conventional methods for disease monitoring.

Therefore, FP-NSA combines speed, specificity, portability, and cost-effectiveness into a promising framework for global surveillance of zoonotic respiratory viruses. The platform is particularly suited for use in resource-limited and hotspot settings where early detection of emerging pathogens is crucial. With ad hoc training and investment, FP-NSA can play a pivotal role in a One Health-aligned, family-wide response to future pandemic threats.

Conclusions

This study demonstrated that the multiplex RT-PCR coupled with Nanopore sequencing enables rapid and accurate detection of targeted viral families in clinical samples within 4 h (from PCR to sequencing and analysis). In addition to detecting a genetically divergent γ-CoV_IBV strain, the assay was effective in detecting viruses in different host species, supporting its applicability for cross-species zoonotic disease surveillance. The portability and adaptability of the MinION platform further enhance the feasibility of deploying this assay in field-based or resource-constrained settings, underscoring its value as a tool for frontline monitoring of emerging and re-emerging pathogens.

Abbreviations

FP-NSA	Family-wide PCR and Nanopore sequencing of amplicons
ONT	Oxford Nanopore Technology
RT-PCR	Reverse transcription PCR
RT-qPCR	Real-time quantitative PCR
α-CoV	Alpha coronavirus
β-CoV	Beta coronavirus

γ-CoV_IBV	Gamma coronavirus infectious bronchitis virus (γ-CoV IBV)
IAV	Influenza A virus
IDV	Influenza D virus
MAFFT	Multiple Alignment using Fast Fourier Transform
SISPA	Sequence-Independent Single Primer Amplification

Supplementary Information

The online version contains supplementary material available at https://doi.org/10.1186/s13073-025-01550-5.

Additional file 1: Table s1 List of primers used in this study. Table s2 Description of the clinical samples included in this study. The selected subset of 78 representative samples from a total of 184 clinical samples and cell culture isolates, used to validate the FP-NSA assay, are highlighted in gray and labeled S1–S78. Neg = negative, Pos = positive, + lw = lower band (< 200 bp), + up = upper band (> 200 bp), + lw/up = double bands (< 200 bp and > 200 bp), + fup = faint upper band (> 200 bp), and N/S + Non-specific bands. Methods s1 Quantification of clinical RNA samples for determining the limit of detection (LoD) of the FP-NSA. Methods s2 Preparation of Nanopore sequencing libraries. Methods s3 In-house bash script-based analysis for Nanopore sequencing data. Methods s4 Sequence-Independent Single Primer Amplification (SISPA) protocol and genome assembly. Fig. s1 Gel image showing the amplification pattern of the targeted respiratory zoonotic viruses using the developed multiplex RT-PCR assay in clinical samples. The samples selected for sequencing by Nanopore MinION device are shown in blue (s1 to s78). Fig. s2 Krona plots showing the taxonomic classification of SISPA reads in sample (A) s66_Botswana and (B) s68_Guinea, using Centrifuge.

Acknowledgements
The authors thank the Veterinary Diagnostic Laboratory (VETLAB) Network partners: Dr. Abel Wade, Laboratoire National Veterinaire (LANAVET), Cameroon, Dr. Nguyen Thi Kim Oanh and Dr. Ngo Van Bac, National Center for Veterinary Diagnosis (NCVD), Vietnam, Dr. Mary Romona Ndanyi, National Veterinary Reference Laboratories, Kabete, Kenya, Dr. Pragya Koirala, Central Veterinary Laboratory, Nepal, Dr. George Dautu Zambia, Central Veterinary Research Institute, Zambia, Dr. Ulaankhuu Ankhanbaatar, State Central Veterinary Laboratory, Mongolia, Dr. Umberto Molini and Dr. Juliet Kabajani, Central Veterinary Laboratory, Namibia, Dr. Samantha L. Letsholo, National Veterinary Laboratory, Botswana, and Mabusetsa Joseph Makalo, Central Veterinary Laboratory, Lesotho, for providing the samples used for this study as well as Dr. Jolanta Kolodziejek, Vetmeduni, Vienna, Austria, for providing the data of the MERS-CoV external quality assessment.

Authors' contributions
Experimental design and conceptualization: IKM, CEL and GC; Data collection and generation: IKM, KBA, WGD and TBKS; Material and positive controls: CL, AS, SRF, FS, LC, KB, KBA and NN; Statistical and bioinformatics analysis: IKM and CEL; Writing—original draft: IKM; Review and/or revision of the manuscript: IKM, KBA, WGD, TBKS, CL, AS, SRF, FS, LC, KB, AM, MD, GC, NN and CEL; Supervision: CEL and GC; Resources and materials: CEL, GC, AM and MD; All authors reviewed and edited the manuscript.

Funding
This work was supported by the VETLAB network initiative of the FAO/IAEA Centre, the IAEA Peaceful Uses Initiative Project, "Detection of Emerging and Re-emerging Animal and Zoonotic Pathogens," funded by the USA and Japan, and the IAEA Coordinated Research Project (CRP) D32039, "Enhancing Laboratory Preparedness for Zoonotic Diseases – ZODIAC in Asia and the Pacific," funded by the Republic of Korea.

Data availability
The partial genome sequence of S68_IBV_Guinea sample is available in the GenBank under the accession number PQ553913, (https://www.ncbi.nlm.nih.gov/nuccore/PQ553913.1/). The SRA data files generated from the metagenomics analysis of s66_Botswana and s68_Guinea samples have been deposited in GenBank under BioSample accession numbers SAMN51157819 and SAMN51157820.

Declarations

Ethics approval and consent to participate
The authors confirm that the ethical policies of the journal, as stated on the journal's ethical guidelines, have been adhered to. The RNA samples from humans were upper respiratory swab samples collected by the Department for Molecular Biology at AGES during a screening program targeting Austrian residential/nursing homes for SARS-CoV-2. The other animal samples used in this study were those stored at the Animal Production and Health Laboratory (APHL), Seibersdorf, Austria, that were initially collected as part of routine diagnosis by the Central/National Veterinary Laboratory of Mauritania, Guinea, Ethiopia, Kuwait, Ivory Coast, Cameroon, Vietnam, Kenya, Nepal, Zambia, Mongolia, Namibia, Botswana, and Lesotho, and submitted to APHL for the characterization of other suspected diseases. The MERS-CoV samples were part of a WHO proficiency test panel, stored at Vetmeduni, Vienna. Ethical approval was not required. This study was conducted in accordance with ARRIVE guidelines.

Consent for publication
Not applicable.

Competing interests
The authors declare no competing interests.

Author details
[1]Animal Production and Health Laboratory, Department of Nuclear Sciences and Applications, Joint FAOIAEA Centre of Nuclear Techniques in Food and AgricultureInternational Atomic Energy Agency, Wagramer Strasse 5, P.O. Box 100, 1400 Vienna, Austria. [2]Cyclotron Applied Research Section, Korea Atomic Energy Research Institute, Jeongeup 56212, Republic of Korea. [3]Institute for Veterinary Disease Control, Austrian Agency for Health and Food Safety (AGES), Robert Koch Gasse 17, 2340 Mödling, Austria. [4]Istituto Zooprofilattico Sperimentale Delle Venezie, Legnaro, Italy. [5]Laboratoire Central Vétérinaire de Diagnostic (LCVD) de Guinée, Conakry 001, Guinea. [6]Food and Agriculture Organization of the United Nations, Viale Delle Terme Di Caracalla, 00153 Rome, Italy. [7]Department of Biological Sciences and Pathobiology, Center of Pathobiology, University of Veterinary Medicine Vienna, Veterinaerplatz 1, 1210 Vienna, Austria. [8]Department of Basic Medical Sciences, College of Medicine, Mohammed Bin Rashid University of Medicine and Health Sciences, Dubai Health, P.O. Box 505055, Dubai, United Arab Emirates.

Received: 15 November 2024 Accepted: 12 September 2025
Published online: 17 October 2025

References

1. Stevenson M, Halpin K, Heuer C. Emerging and endemic zoonotic diseases: surveillance and diagnostics. OIE Rev Sci Tech. 2021;40.
2. Rahman MT, Sobur MA, Islam MS, Ievy S, Hossain MJ, Zowalaty MEE, et al. Zoonotic diseases: etiology, impact, and control. Microorganisms. 2020. https://doi.org/10.3390/microorganisms8091405.
3. World Health Organization. Influenza (avian and other zoonotic). WHO. 2018; January.
4. Çelik İ, Saatçi E, Eyüboğlu FÖ. Emerging and reemerging respiratory viral infections up to COVID-19. Turkish Journal of Medical Sciences. 2020;50 SI-1.
5. Rosenberg R. Detecting the emergence of novel, zoonotic viruses pathogenic to humans. Cell Mol Life Sci. 2015. https://doi.org/10.1007/s00018-014-1785-y.
6. Kreuder Johnson C, Hitchens PL, Smiley Evans T, Goldstein T, Thomas K, Clements A, et al. Spillover and pandemic properties of zoonotic viruses with high host plasticity. Sci Rep. 2015. https://doi.org/10.1038/srep14830.
7. Karron RA, Black RE. Determining the burden of respiratory syncytial virus disease: the known and the unknown. Lancet. 2017. https://doi.org/10.1016/S0140-6736(17)31476-9.
8. Khalil AM, Martinez-Sobrido L, Mostafa A. Zoonosis and zooanthroponosis of emerging respiratory viruses. Frontiers in Cellular and Infection Microbiology. 2023;13.

9. Sreenivasan CC, Thomas M, Kaushik RS, Wang D, Li F. Influenza a in bovine species: a narrative literature review. Viruses. 2019;11.
10. Shereen MA, Khan S, Kazmi A, Bashir N, Siddique R. COVID-19 infection: origin, transmission, and characteristics of human coronaviruses. Journal of Advanced Research. 2020;24.
11. ZHANG LL, ZHANG C, PENG JP. Application of Nanopore sequencing technology in the clinical diagnosis of infectious diseases. Biomedical and Environmental Sciences. 2022;35.
12. Boukli N, Flamand C, Chea KL, Heng L, Keo S, Sour K, et al. One assay to test them all: multiplex assays for expansion of respiratory virus surveillance. Front Med. 2023. https://doi.org/10.3389/fmed.2023.1161268.
13. Allen T, Murray KA, Zambrana-Torrelio C, Morse SS, Rondinini C, Di Marco M, et al. Global hotspots and correlates of emerging zoonotic diseases. Nat Commun. 2017. https://doi.org/10.1038/s41467-017-00923-8.
14. Hassan OA, de Balogh K, Winkler AS. One Health early warning and response system for zoonotic diseases outbreaks: emphasis on the involvement of grassroots actors. Vet Med Sci. 2023;9.
15. Kanzi AM, San JE, Chimukangara B, Wilkinson E, Fish M, Ramsuran V, et al. Next generation sequencing and bioinformatics analysis of family genetic inheritance. Front Genet. 2020. https://doi.org/10.3389/fgene.2020.544162.
16. Zhu X, Yan S, Yuan F, Wan S. The applications of Nanopore sequencing technology in pathogenic microorganism detection. Can J Infect Dis Med Microbiol. 2020;2020.
17. Millar D, Melki J. Diagnosis of viral families using a nucleic acid simplification technique. 2023.
18. van Boheemen S, Bestebroer TM, Verhagen JH, Osterhaus ADME, Pas SD, Herfst S, et al. A family-wide rt-pcr assay for detection of paramyxoviruses and application to a large-scale surveillance study. PLoS One. 2012;7.
19. Wacharapluesadee S, Buathong R, Iamsirithawon S, Chaifoo W, Ponpinit T, Ruchisrisarod C, et al. Identification of a novel pathogen using family-wide PCR: initial confirmation of COVID-19 in Thailand. Front Public Health. 2020. https://doi.org/10.3389/fpubh.2020.555013.
20. WHO. Pathogens prioritization: a scientific framework for epidemic and pandemic research preparedness. 2024.
21. Untergasser A, Cutcutache I, Koressaar T, Ye J, Faircloth BC, Remm M, et al. Primer3-new capabilities and interfaces. Nucleic Acids Res. 2012. https://doi.org/10.1093/nar/gks596.
22. Pas SD, Patel P, Reusken C, Domingo C, Corman VM, Drosten C, et al. First international external quality assessment of molecular diagnostics for MERS-CoV. J Clin Virol. 2015;69.
23. Fereidouni SR, Harder TC, Gaidet N, Ziller M, Hoffmann B, Hammoumi S, et al. Saving resources: avian influenza surveillance using pooled swab samples and reduced reaction volumes in real-time RT-PCR. J Virol Methods. 2012. https://doi.org/10.1016/j.jviromet.2012.08.002.
24. Takemura T, Ankhanbaatar U, Settypalli TBK, Purevtseren D, Shura G, Damdinjav B, et al. SARS-CoV-2 infection in beaver farm, Mongolia, 2021. Emerg Infect Dis. 2024;30.
25. Hoffmann B, Hoffmann D, Henritzi D, Beer M, Harder TC. Riems influenza a typing array (RITA): an RT-qPCR-based low density array for subtyping avian and mammalian influenza a viruses. Sci Rep. 2016;6.
26. Muradrasoli S, Mohamed N, Hornyák Á, Fohlman J, Olsen B, Belák S, et al. Broadly targeted multiprobe QPCR for detection of coronaviruses: coronavirus is common among mallard ducks (*Anas platyrhynchos*). J Virol Methods. 2009. https://doi.org/10.1016/j.jviromet.2009.04.022.
27. Corman VM, Eckerle I, Bleicker T, Zaki A, Landt O, Eschbach-Bludau M, et al. Detection of a novel human coronavirus by real-time reverse-transcription polymerase chain reaction. Eurosurveillance. 2012;17.
28. Rume VN, Dundon WG, Belay G, Baziki J de D, Diakite A, Paul A, et al. Molecular epidemiological update of peste des petits ruminants virus (PPRV) in Ethiopia. Vet Microbiol. 2019;235.
29. Chrzastek K, Lee D, Smith D, Sharma P, Suarez DL, Pantin-Jackwood M, et al. Use of sequence-independent, single-primer-amplification (SISPA) for rapid detection, identification, and characterization of avian RNA viruses. Virology. 2017. https://doi.org/10.1016/j.virol.2017.06.019.
30. Letunic I, Bork P. Interactive tree of life (iTOL) v5: an online tool for phylogenetic tree display and annotation. Nucleic Acids Res. 2021;49:W293–6.
31. Faccini S, De Mattia A, Chiapponi C, Barbieri I, Boniotti MB, Rosignoli C, et al. Development and evaluation of a new real-time RT-PCR assay for detection of proposed influenza D virus. J Virol Methods. 2017. https://doi.org/10.1016/j.jviromet.2017.01.019.
32. Ito T, Gorman OT, Kawaoka Y, Bean WJ, Webster RG. Evolutionary analysis of the influenza A virus M gene with comparison of the M1 and M2 proteins. J Virol. 1991. https://doi.org/10.1128/jvi.65.10.5491-5498.1991.
33. Woo PCY, Huang Y, Lau SKP, Yuen KY. Coronavirus genomics and bioinformatics analysis. Viruses. 2010. https://doi.org/10.3390/v2081803.
34. Wang Y, Zhao Y, Bollas A, Wang Y, Au KF. Nanopore sequencing technology, bioinformatics and applications. Nat Biotechnol. 2021. https://doi.org/10.1038/s41587-021-01108-x.
35. Relova D, Rios L, Acevedo AM, Coronado L, Perera CL, Pérez LJ. Impact of RNA degradation on viral diagnosis: an understated but essential step for the successful establishment of a diagnosis network. Vet Sci. 2018. https://doi.org/10.3390/vetsci5010019.
36. Parker J, Fowler N, Walmsley ML, Schmidt T, Scharrer J, Kowaleski J, et al. Analytical sensitivity comparison between singleplex real-time PCR and a multiplex PCR platform for detecting respiratory viruses. PLoS One. 2015;10.
37. Wang X, Huang Z, Song J, Xiao Y, Wang H. Analytical sensitivity comparison of 14 conventional and three rapid RT-PCR assays for SARS-CoV-2 detection. J Virol Methods. 2021;293.
38. Marandino A, Mendoza-González L, Panzera Y, Tomás G, Williman J, Techera C, et al. Genome variability of infectious bronchitis virus in Mexico: high lineage diversity and recurrent recombination. Viruses. 2023. https://doi.org/10.3390/v15071581.
39. Butler KS, Carson BD, Podlevsky JD, Mayes CM, Rowland JM, Campbell DA, et al. Singleplex, multiplex and pooled sample real-time RT-PCR assays for detection of SARS-CoV-2 in an occupational medicine setting. Sci Rep. 2022. https://doi.org/10.1038/s41598-022-22106-2.
40. Hao X, Liu R, He Y, Xiao X, Xiao W, Zheng Q, et al. Multiplex PCR methods for detection of several viruses associated with canine respiratory and enteric diseases. PLoS ONE. 2019. https://doi.org/10.1371/journal.pone.0213295.
41. Gómez de la Torre Pretell JC, Hueda-Zavaleta M, Cáceres-DelAguila JA, Barletta-Carrillo C, Copaja-Corzo C, Poccorpachi M del PS, et al. Clinical characteristics associated with detected respiratory microorganism employing multiplex nested PCR in patients with presumptive COVID-19 but negative molecular results in Lima, Peru. Trop Med Infect Dis. 2022;7.
42. Yelagandula R, Bykov A, Vogt A, Heinen R, Özkan E, Strobl MM, et al. Multiplexed detection of SARS-CoV-2 and other respiratory infections in high throughput by SARSeq. Nat Commun. 2021;12.
43. MacKenzie M, Argyropoulos C. An introduction to Nanopore sequencing: past, present, and future considerations. Micromachines. 2023;14.
44. Runtuwene LR, Tuda JSB, Mongan AE, Suzuki Y. On-site MinION sequencing. In: Advances in experimental medicine and biology. 2019.
45. Chen P, Sun Z, Wang J, Liu X, Bai Y, Chen J, et al. Portable nanopore-sequencing technology: trends in development and applications. Front Microbiol. 2023. https://doi.org/10.3389/fmicb.2023.1043967.
46. Lamb HJ, Hayes BJ, Nguyen LT, Ross EM. The future of livestock management: a review of real-time portable sequencing applied to livestock. Genes. 2020;11.
47. Gavina K, Franco LC, Khan H, Lavik JP, Relich RF. Molecular point-of-care devices for the diagnosis of infectious diseases in resource-limited settings – a review of the current landscape, technical challenges, and clinical impact. J Clin Virol. 2023. https://doi.org/10.1016/j.jcv.2023.105613.
48. Srivathsan A, Meier R. Scalable, cost-effective, and decentralized DNA barcoding with Oxford Nanopore sequencing. In: DeSalle R, editor. DNA barcoding: methods and protocols. New York, NY: Springer US; 2024. p. 223–38.
49. Petersen LM, Martin IW, Moschetti WE, Kershaw CM, Tsongalis GJ. Third-generation sequencing in the clinical laboratory: exploring the advantages and challenges of nanopore sequencing. Journal of Clinical Microbiology. 2020;58.

Publisher's Note